

Experimental validation of collective circular motion for nonholonomic multi-vehicle systems

Daniele Benedettelli, Nicola Ceccarelli, Andrea Garulli,
Antonio Giannitrapani

*Dipartimento di Ingegneria dell'Informazione
Università di Siena
Via Roma, 56
53100 Siena - ITALY*

Abstract

This paper presents the experimental validation of a recently proposed decentralized control law, for the collective circular motion of a team of nonholonomic vehicles about a virtual reference beacon. The considered control strategy ensures global asymptotic stability in the single-vehicle case and local asymptotic stability in the multi-vehicle scenario. The main contribution of this work is to evaluate the performance of the proposed algorithm in presence of a number of uncertainty sources naturally arising in a real-world environment. Both static and moving reference beacon are considered, in a low-cost experimental framework based on the LEGO MINDSTORMS technology. The adopted setup features good scalability and is versatile enough to be adopted for the evaluation of different control strategies. At the same time, it represents a challenging testbed, exhibiting several issues that have to be faced in real-world applications.

Key words: Collective motion, experimental validation, distributed control law.

1 Introduction

In recent years multi-agent systems have received considerable attention for their potential in many different fields. It is a matter of fact that a team of autonomous agents can lead to more efficient solutions to many problems arising in exploration of unknown or hostile environments, surveillance of large areas, distributed monitoring, to name just a few. A multi-agent system features shorter task completion time, reduced costs (a team of simple robots is

less expensive than a single complex robot), increased reliability (robustness to failures). However, in order to fully exploit the potential of such systems, suitable distributed algorithms, relying only on the information locally available to each agent, have to be devised. A common problem to be faced for the successful employment of a team of vehicles is motion coordination. The control law of each agent has to be designed so as to achieve a desired collective motion of the team, while at the same time avoiding collisions. In the last decade several solutions to this problem have been proposed, for different vehicle motion models. Although a rigorous stability analysis of control laws for multi-agent systems is generally a difficult task, nice theoretical results have been obtained both in the case of linear models [1–3] and in the more challenging scenario of nonholonomic vehicles [4–6]. On the other hand, most of the proposed algorithms have been tested only in simulation and relatively few experimental results can be found in the literature [7–10].

The contribution of this paper is twofold. First, it presents results on the experimental validation of a recently proposed decentralized control law, for the collective circular motion of a group of agents [11,12]. The objective of the team is to achieve counterclockwise rotation about a reference beacon. The considered control strategy ensures global asymptotic stability in the single-vehicle case and local asymptotic stability in the multi-vehicle scenario, with respect to a static beacon. Several experiments featuring a moving reference beacon are also reported. As a second contribution, the paper describes a low-cost experimental setup, based on the LEGO MINDSTORMS technology, which can be of interest for the performance evaluation of different control schemes for collective motion of multi-vehicle systems. The adopted technology exhibits some severe limitations, in terms of computing power, communication resources and actuator precision, thus making the collective motion problem even more challenging. A preliminary version of this work has been presented in [13].

The paper is structured as follows. In Section 2 the collective circular motion problem, for a team of unicycle-like vehicles is stated. Section 3 introduces the decentralized control law to be validated and summarizes its theoretical properties. Section 4 presents an overview of the experimental setup used to evaluate the performance of the proposed control strategy. Experimental results are reported in Section 5, while in Section 6 some conclusions are drawn.

2 Problem formulation

Let us consider a group of n agents whose motion is described by the kinematic equations

$$\begin{aligned}
\dot{x}_i &= v \cos \theta_i \\
\dot{y}_i &= v \sin \theta_i \\
\dot{\theta}_i &= u_i,
\end{aligned}
\quad i = 1, \dots, n \tag{1}$$

where $[x_i \ y_i \ \theta_i] \in \mathbb{R}^2 \times [-\pi, \pi)$ represents the i -th agent pose, v is the forward speed (assumed to be constant) and u_i is the angular speed, which plays the role of control input for vehicle i . Each vehicle is supposed to be equipped with a sensory system providing range and bearing measurements with respect to: i) a virtual reference beacon, and ii) all its neighbors. Specifically, with reference to the i -th agent, (ρ_i, γ_i) will denote the measurements with respect to the beacon, while (ρ_{ij}, γ_{ij}) will denote the measurement with respect to the j -th agent (see Figure 1).

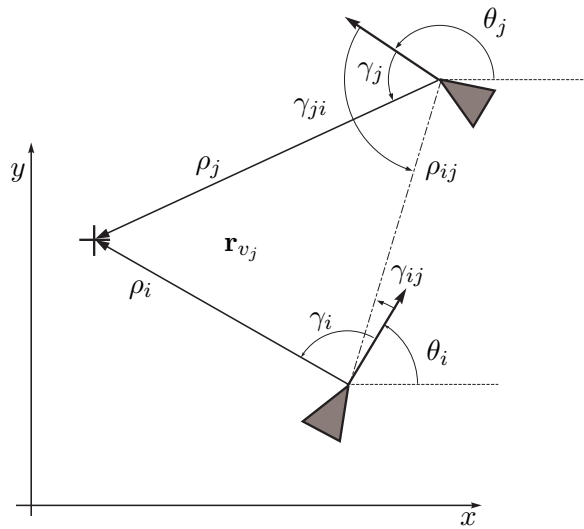


Fig. 1. Two vehicles (triangles) and a beacon (cross).

In order to explicitly take into account sensor limitations, a *visibility region* \mathcal{V}_i is defined for each agent, representing the region where it is assumed that the sensors of the i -th vehicle can perceive its neighbors. In this paper, the visibility region has been chosen as the union of two sets (see Figure 2):

- A circular sector of radius d_l and angular amplitude $2\alpha_v$, centered at the vehicle. It models the presence of a long range sensor with limited angular visibility (e.g., a laser range finder).
- A circular region around the vehicle of radius d_s , which models a proximity sensor (e.g., a ring of sonars) and plays the role of a “safety region” around the vehicle.

This means that the measurements (ρ_{ij}, γ_{ij}) are available to the i -th agent if and only if one of the following conditions is verified: (i) $|\rho_{ij}| \leq d_l$ and

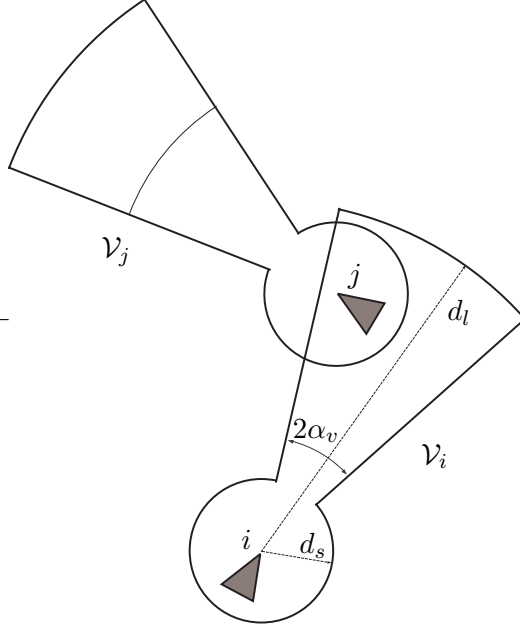


Fig. 2. Visibility region of i -th and j -th vehicle.

$|\beta_d(\gamma_{ij})| \leq \alpha_v$; (ii) $|\rho_{ij}| \leq d_s$, where

$$\beta_d(\gamma_{ij}) = \begin{cases} \gamma_{ij} & \text{if } 0 \leq \gamma_{ij} \leq \pi \\ \gamma_{ij} - 2\pi & \text{if } \pi < \gamma_{ij} < 2\pi. \end{cases} \quad (2)$$

The objective is to design the control inputs u_i so that all the agents achieve circular motion around the beacon, with prescribed radius of rotation and distances between neighbors, while at the same time avoiding collisions. In the next section, a decentralized control law addressing this problem is briefly described.

3 Decentralized control law

In order to illustrate the control law to be validated, let \mathcal{N}_i be the set containing the indexes of the vehicles that lie inside the visibility region \mathcal{V}_i of the i -th agent. The proposed control law computes the input $u_i(t)$ as

$$u_i(t) = f_{ib}(\rho_i, \gamma_i) + \sum_{j \in \mathcal{N}_i(t)} f_{ij}(\rho_{ij}, \gamma_{ij}), \quad (3)$$

where

$$f_{ib}(\rho_i, \gamma_i) = \begin{cases} k_b \cdot g(\rho_i; c_b, \rho_0) \cdot \alpha_d(\gamma_i; \psi) & \text{if } \rho_i > 0 \\ 0 & \text{if } \rho_i = 0, \end{cases} \quad (4)$$

$$f_{ij}(\rho_{ij}, \gamma_{ij}) = \begin{cases} k_v \cdot g(\rho_{ij}; c_v, d_0) \cdot \beta_d(\gamma_{ij}) & \text{if } \rho_{ij} > 0 \\ 0 & \text{if } \rho_{ij} = 0. \end{cases} \quad (5)$$

The functions $g(\cdot)$ and $\alpha_d(\cdot)$ in (4) and (5) are defined as

$$g(\rho; c, \xi) = \ln \left(\frac{(c-1) \cdot \rho + \xi}{c \cdot \xi} \right) \quad (6)$$

$$\alpha_d(\gamma; \psi) = \begin{cases} \gamma(t) & \text{if } 0 \leq \gamma(t) \leq \psi \\ \gamma(t) - 2\pi & \text{if } \psi < \gamma(t) < 2\pi, \end{cases} \quad (7)$$

where $c > 1$, $\xi > 0$, and $\psi \in (\frac{3}{2}\pi, 2\pi)$ are given constants. The term $g(\rho; c, \xi)$ has to be intended as a smoothing function that scales the angular velocity according to the distance ρ to the beacon, while ensuring to remain bounded as ρ tends to zero. Notice that for $c > 1$ the function $g(\rho; c, \xi)$ is positive if and only if $\rho > \xi$. The function $\beta_d(\gamma_{ij})$ has been defined in (2), while $k_b > 0$ and $k_v > 0$ are the controller parameters. The parameter d_0 is the desired distance between two consecutive vehicles when rotating about the beacon. The radius d_s of the safety circle around a vehicle is always supposed to be smaller than the desired inter-vehicle distance d_0 .

The control law (3) is the result of two contributions, with different objectives. Each agent i is driven by the term $f_{ib}(\cdot)$ towards the counterclockwise circular motion about the beacon. The terms $f_{ij}(\cdot)$ have a twofold aim: to enforce $\rho_{ij} = d_0$ for all the agents $j \in \mathcal{N}_i$ and, at the same time, to favor collision-free trajectories. Indeed, the i -th vehicle is attracted by any vehicle $j \in \mathcal{N}_i$ if $\rho_{ij} > d_0$, and repulsed if $\rho_{ij} < d_0$. Moreover, since $d_s < d_0$, the term $g(\rho_{ij}; c_v, d_0)$ in (5) is always negative for $\rho_{ij} < d_s$, thus pushing the j -th agent outside the circular safety region around the i -th vehicle and therefore hindering collisions among the vehicles. The aim of such combined actions is to make the agents safely reach the counterclockwise circular motion, with distance d_0 between consecutive vehicles. Notice that the sets \mathcal{N}_i are time-varying, which implies that the control law (3) switches every time a vehicle enters into or exits from the region \mathcal{V}_i .

Another appealing feature of the control law (3)-(5) is that when a vehicle is faraway from the beacon, it is forced to point towards the beacon and track it in rectilinear motion. In fact, when a vehicle is far from the beacon, then $\rho_i \gg \rho_{ij}$ for each $j \in \mathcal{N}_i$, and the function $f_{ib}(\cdot)$ dominates the terms $f_{ij}(\cdot)$, i.e. $u_i \simeq f_{ib}(\rho_i, \gamma_i)$. Since $g(\rho_i; c_b, \rho_0) > 0$ when ρ_i is large, the effect of the control input u_i is to drive to zero the angle γ_i , i.e. to steer the vehicle towards the beacon. This suggests that it is not necessary to switch to a different control law when the beacon is far or it is moved to another location.

Some theoretical results have been provided for this control law. The proofs

of such results are given in [11,12]. The first one concerns the single-vehicle case, and can be summarized as follows.

Result 1 *Let $n = 1$. If the control parameters k_b, c_b, ρ_0 are chosen such that*

$$\min_{\rho} \rho \cdot g(\rho; c_b, \rho_0) > -\frac{2v}{3\pi k_b}, \quad (8)$$

then the counterclockwise rotation about the beacon with rotational radius ρ_e defined as the unique solution of

$$\frac{v}{\rho_e} - k_b \cdot g(\rho_e; c_b, \rho_0) \cdot \frac{\pi}{2} = 0 \quad (9)$$

and angular velocity $\frac{v}{\rho_e}$, is a globally asymptotically stable limit cycle for the system (1) with the control law (3).

The above result basically states that in the single-vehicle case, the control law $u_i = f_{ib}$ results in the counterclockwise rotation of the vehicle about the beacon, with radius ρ_e , for every initial robot pose.

For the multi-vehicle case, a sufficient condition has been derived which guarantees the local asymptotic stability of a family of team configurations corresponding to the collective circular motion about the beacon.

Result 2 *Let $\alpha_v \leq \frac{\pi}{2}$, and assume that (8) holds. If the controller parameters satisfy $d_s < d_0 < d_l$ and*

$$(n-1) \arcsin\left(\frac{d_0}{2\rho_e}\right) + \varphi < \pi \quad (10)$$

$$2 \arcsin\left(\frac{d_0}{2\rho_e}\right) > \varphi \quad (11)$$

*where*¹

$$\varphi = \min\left\{\alpha_v, \arcsin\left(\frac{d_l}{2\rho_e}\right)\right\} \quad (12)$$

then every configuration of n vehicles in counterclockwise circular motion around a fixed beacon, with rotational radius $\rho_i = \rho_e$ defined in (9), $\gamma_i = \frac{\pi}{2}$ and $\rho_{ij} = d_0 \forall i = 1 \dots n$ and $\forall j \in \mathcal{N}_i$, corresponds to a limit cycle for the system (1) with the control law (3). Moreover, if

$$\frac{k_v}{k_b} \leq 2 \frac{c_v}{c_b} \frac{c_b - 1}{c_v - 1}, \quad (13)$$

then the aforementioned limit cycles are locally asymptotically stable.

¹ With a slight abuse of notation, it is meant that $\varphi = \alpha_v$ whenever $d_l > 2\rho_e$.

The inequality in (10) guarantees that the n vehicles can lie on a circle of radius ρ_e , with distance d_0 between two consecutive vehicles and with at least one vehicle that does not perceive any other vehicle. The inequality (11) ensures that at equilibrium, a vehicle cannot perceive more than one vehicle within its visibility region (see Figure 3). In (10)-(11), φ represents the maximum angular distance γ_{ij} such that the i -th vehicle perceives the j -th one, when the two vehicles are moving in circular motion with rotational radius ρ_e .

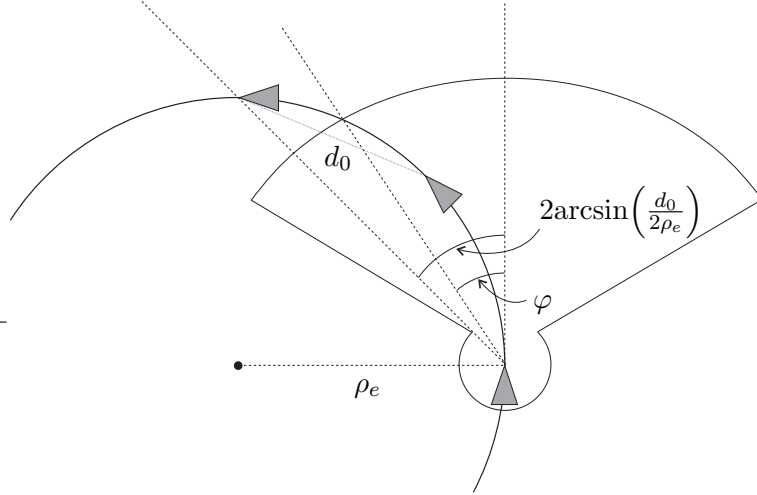


Fig. 3. Three vehicles in an equilibrium configuration satisfying condition (11). Notice that in this example $\varphi = \arcsin\left(\frac{d_0}{2\rho_e}\right)$.

When (10) is satisfied, there can be several different equilibrium configurations, all corresponding to collective circular motion about the beacon. Indeed, an equilibrium configuration can be in general composed of q separate platoons, each one containing consecutive vehicles at distance d_0 . The limit cases are obviously $q = 1$ (a unique platoon) and $q = n$ (n vehicles rotating independently about the beacon). A key point of the proposed approach is that the decentralized control strategy does not aim at enforcing one specific equilibrium configuration (as it occurs, e.g., in cyclic pursuit schemes), but is satisfied with the vehicles ending up in circular motion at the prescribed distance ρ_e from the beacon, while maintaining a minimum distance d_0 between them.

It is worth noticing that this control law does not require exteroceptive orientation measurements, nor labeling of the vehicles. Each agent can compute its control input from range and bearing measurements, without any exchange of information.

It is always possible to select the control law parameters so that the constraints (8), (10), (11) and (13) are satisfied. The parameter ρ_0 must be sufficiently small to verify inequality (8), but sufficiently large to make the radius

ρ_e large enough to satisfy the inequality (10). On the other hand, since ρ_e can be increased by suitably reducing k_b , it is always possible to find a sufficiently small k_b satisfying both (8) and (10). However, a too small k_b may lead to violation of the sufficient condition (13), and hence stability of the desired circular collective motion is not guaranteed anymore. Similarly, the choice of k_v is driven by a trade-off between safety and stability. The choice of a small k_v is motivated by the stability constraint (13), while a large k_v favors safe trajectories by increasing repulsion between nearby vehicles. The shaded area in Figure 4 represents the region of feasible parameters k_b and ρ_0 , for the experimental setup presented in Section 5.1 (Experiment B). The region below the upper dashed curve contains the values of k_b and ρ_0 satisfying (8). The constraint (10) is satisfied by all the pairs (k_b, ρ_0) above the bottom dashed line (constraint (11) turns out to be always satisfied in this setup). Finally, the sufficient condition (13) is satisfied by all values of k_b lying on the right of the vertical dashed line (notice that for $c_b = c_v$, condition (13) simplifies to $k_b \geq \frac{k_v}{2}$). A detailed discussion on the control parameter design is reported in [12].

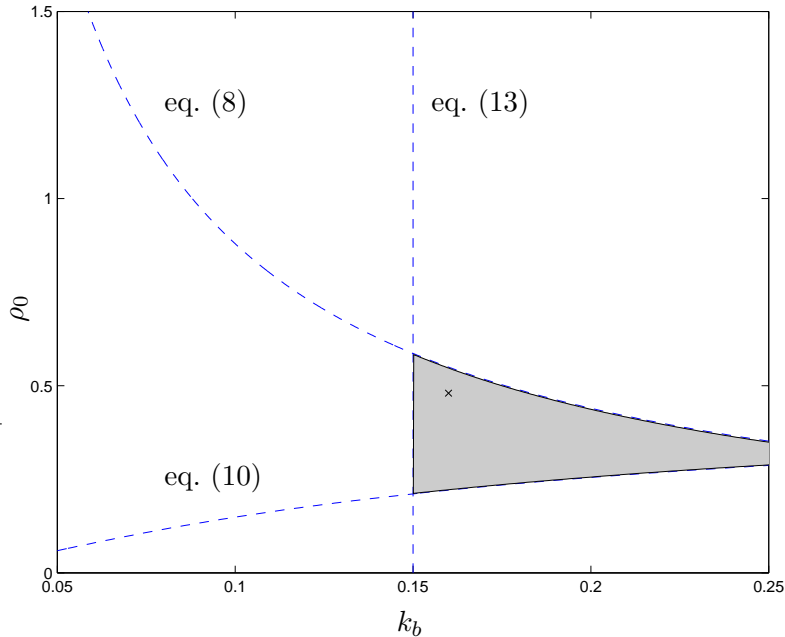


Fig. 4. Feasible region for parameters k_b and ρ_0 for the experimental setup of Section 5.1. The cross denotes the value chosen for Experiment B.

4 Experimental setup

In order to test the performance of the proposed control law in a real-world scenario, a team of mobile robots based on the LEGO MINDSTORMS technology [14] has been employed. All the robots are identical, except for a triangular

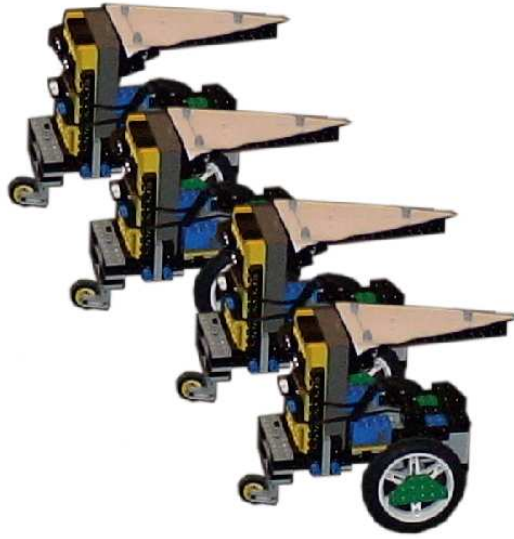


Fig. 5. MINDSTORMS mobile team.

marker placed on the top of each vehicle, whose purpose is to allow a Centralized Supervision System (CSS) to detect the agent identity, and estimate their position and orientation.

The robots have a differential drive kinematics and are driven by two motors, with an idle wheel acting as third support (see Figure 5). Such nonholonomic vehicles can be modeled as unicycles, according to (1), where the linear speed v and the angular speed u represent the control inputs. The motors drive the wheels with a 9:1 gear ratio, while the encoders are coupled to the motors with a 1:5 gear ratio, thus ensuring enough torque and a good encoder resolution (720 ticks per wheel revolution).

Each vehicle is controlled by a LEGO RCX programmable brick [15] equipped with a 16-bit 10Mhz H8/3292 Hitachi processor. The BrickOS real-time operating system [16] allows one to run C/C++ programs to control the motors with 255 PWM levels, to read sensors and to communicate with the CSS via an IR serial protocol. BrickOS also defines its own wireless communication protocol called LNP (LegOS Network Protocol [17]).

The information provided by the onboard encoders is used by the RCX for controlling the wheel speed ω . For each wheel, a two degrees of freedom controller is implemented to track the wheel speed references ω_d provided by the CSS. A PI feedback control is coupled with a feed-forward action $f(\cdot)$, based on the estimated characteristic between the RCX PWM output and the wheel speed (see Figure 6). Due to technological limitations (e.g., RCX numerical approximations, mechanical dead zones) vehicles cannot have a nonzero angular speed less than 0.05 rad/s , while the maximum achievable linear speed

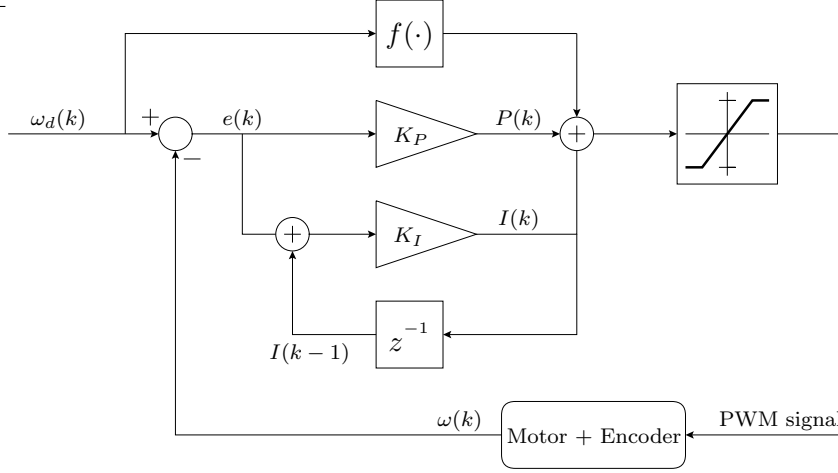


Fig. 6. Motor control scheme.

is about 0.07 m/s .

The Centralized Supervision System is used to monitor the robots during the experiments (see Figure 7). A camera fixed on the lab ceiling is used to capture the motion of the vehicles and to simulate the presence of onboard sensors. Robot position, orientation and identity are detected thanks to white triangles placed on each of them. The overall image processing is illustrated in Figure 8. The original image is captured at a resolution of 640×480 pixels (see Figure 8(a), where white spots represent disturbances due to ambient light). After discarding color information and applying a brightness threshold, a black and white image is obtained (Figure 8(b)). Then, the boundaries of the objects present in the scene are extracted and filtered according to their shape and area. In this stage, artifacts due to light reflections are removed (Figure 8(c)). The position and orientation of a robot are estimated as the center of mass and the orientation of the corresponding triangle (Figure 8(d)). As a byproduct, a unique identity is given to each robot on the basis of the area of the corresponding triangle (i.e., the first robot is the one associated with the smallest triangle and the last one is the vehicle labeled with the largest triangle). Finally, range and bearing measurements $\rho_i, \gamma_i, \rho_{ij}, \gamma_{ij}$ with respect to the virtual reference beacon and the robot neighbors, required by the control law (3), are computed from the position and orientation data previously extracted.

Image capture and processing, as well as the computation of the control law are carried out by a MATLAB script, which also sends speed references to the team via an IR LEGO Tower, interfaced to MATLAB through a MEX DLL written on purpose. The control law output commands are represented as floating point numbers, and need to be converted to 16-bit integers before being sent, in order to keep a good precision for on-robot integer arithmetic calculations. The commands for all robots are packed together and broadcast

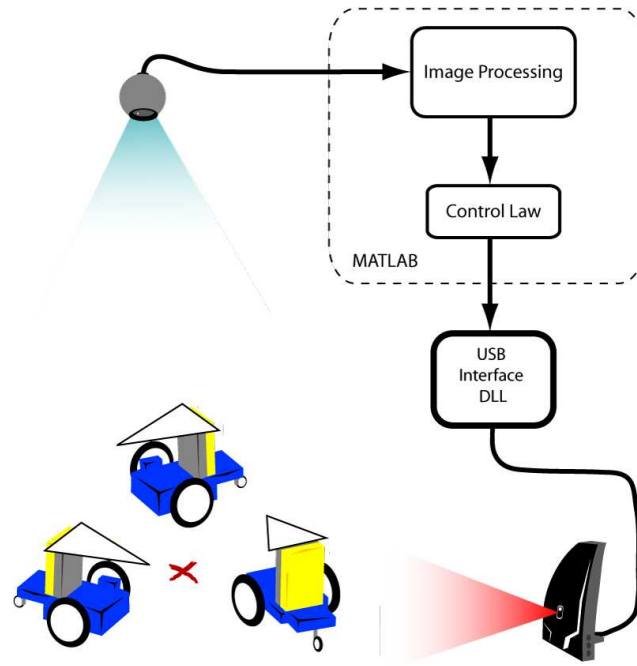


Fig. 7. Centralized Supervision System.

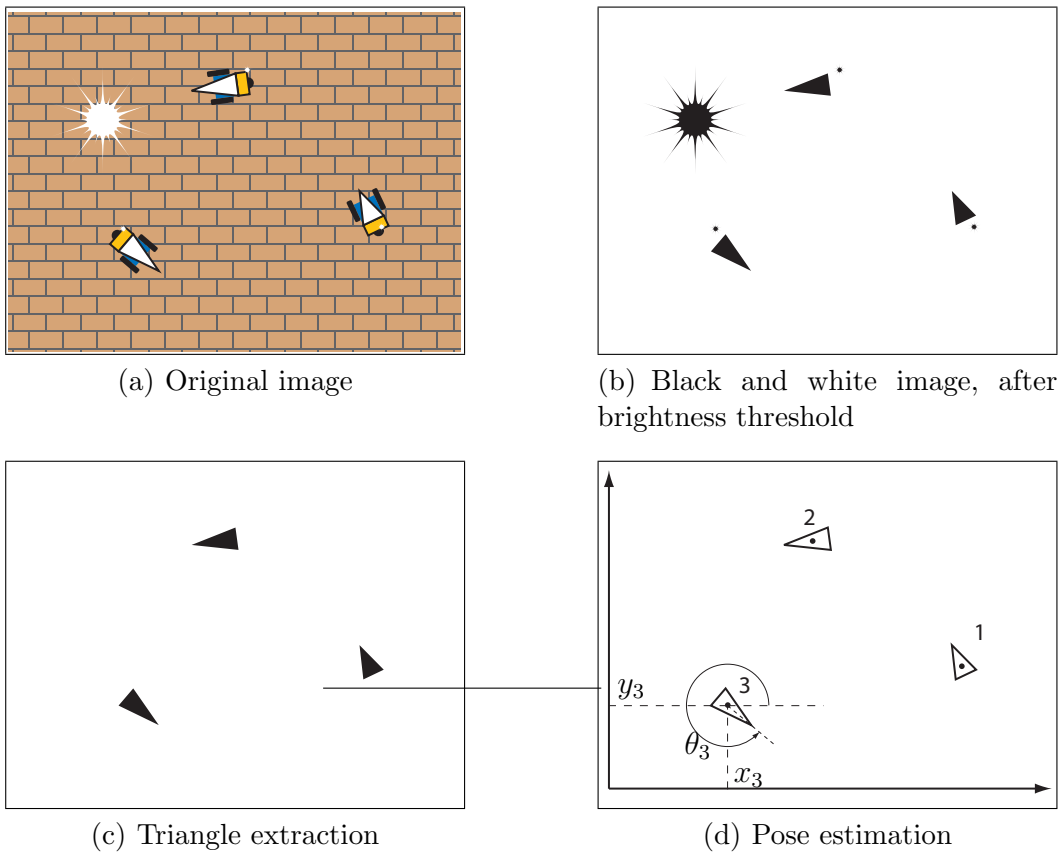


Fig. 8. Image processing

to all vehicles at each sampling time. At the beginning of the experiment each vehicle is given an ID number according to its triangular marker, so that when a robot receives the packet, it is able to recognize which chunk contains its own data.

The centralized architecture described above has two main purposes. First, the CSS is used to simulate the presence of onboard sensors, thus reducing the cost of the experimental setup. Secondly, all the computations can be done on a standard PC, without overloading the vehicle RCX, which is exclusively devoted to the motor control. Additionally, the CSS provides also the ground truth of each vehicles, which allows one to reconstruct the collective motion of the team. Nonetheless, it must be remarked that the tested control law is completely decentralized. In the experiments, the input of each agent is computed by the CSS on the basis of the sole measurements the agent would have access to, if it was equipped with a proper sensory system. Analogously, as far as the control law is concerned, vehicles need not to be distinguishable. They are labeled only to allow them to extract the correct input command from the packet sent by the CSS.

5 Experimental results

In this section, results of experimental tests involving different number of vehicles are reported. The forward speed is set to $v = 0.06 \text{ m/s}$. Range and bearing measurements are extracted from the images taken by the ceiling camera, simulating on-board range sensors (e.g., a laser rangefinder or a ring of sonars). To account for sensor limited field of view, a visibility region like that presented in Section 2 is assumed, with $d_l = 1 \text{ m}$ and $d_s = 0.3 \text{ m}$. The angular width α_v has been set to different values in order to simulate different sensors (see Figure 2).

5.1 Static beacon

In a first set of tests featuring two vehicles with $\alpha_v = \pi/2$ (Experiment A), the following controller parameters have been used (see Section 3): $\psi = 290^\circ$, $k_b = 0.16$, $\rho_0 = 0.3 \text{ m}$, $c_b = 2$, $k_v = 0.3$, $d_0 = 0.6 \text{ m}$, $c_v = 2$. This choice of k_b and ρ_0 satisfies all the stability constraints and corresponds to a desired circular motion of radius $\rho_e = 0.6 \text{ m}$, while d_0 models a desired displacement between vehicles in circular motion of 0.6 m . In Figure 9 the vehicle paths (dashed lines) of a typical experiment are depicted. Filled triangles correspond to the vehicle initial poses, while empty triangles represent the vehicle poses at the end of the run. After a transient (whose duration depends on the initial

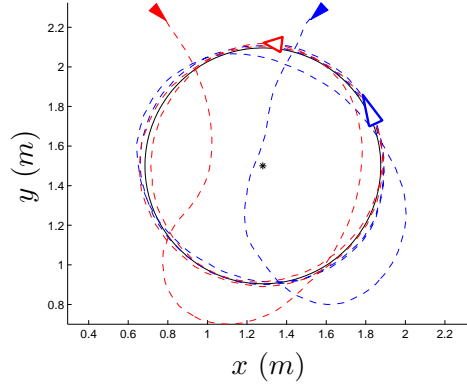


Fig. 9. Experiment A: Vehicle paths (dashed lines) and desired circular path (solid line) about the beacon (asterisk). Filled triangles represent the vehicle initial poses, empty triangles are the final vehicle poses.

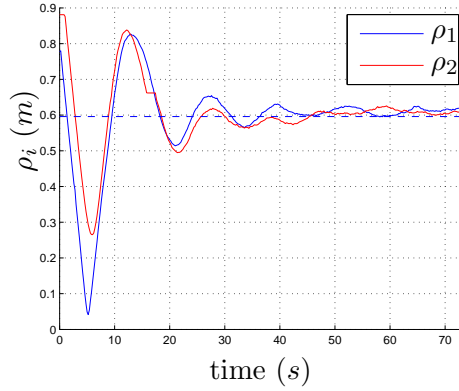


Fig. 10. Experiment A: Actual distances ρ_1 , ρ_2 of the vehicles to the beacon (solid lines) and desired radius $\rho_e = 0.6$ (dashed line).

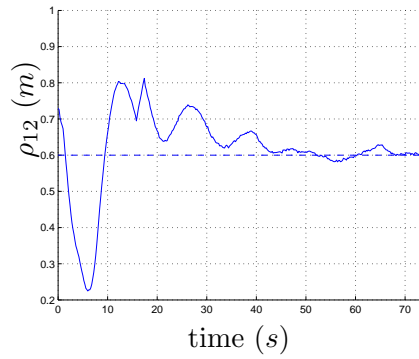


Fig. 11. Experiment A: Actual distance ρ_{12} between the vehicles (solid line) and desired one $d_0 = 0.6$ (dashed line).

conditions) both trajectories approach a circle of radius ρ_e , and the vehicle separation settles about d_0 . This appears clearly in Figures 10-11, where the distances of the agents from the beacon and the inter-vehicle distance are shown, respectively. One can observe that this control strategy is actually

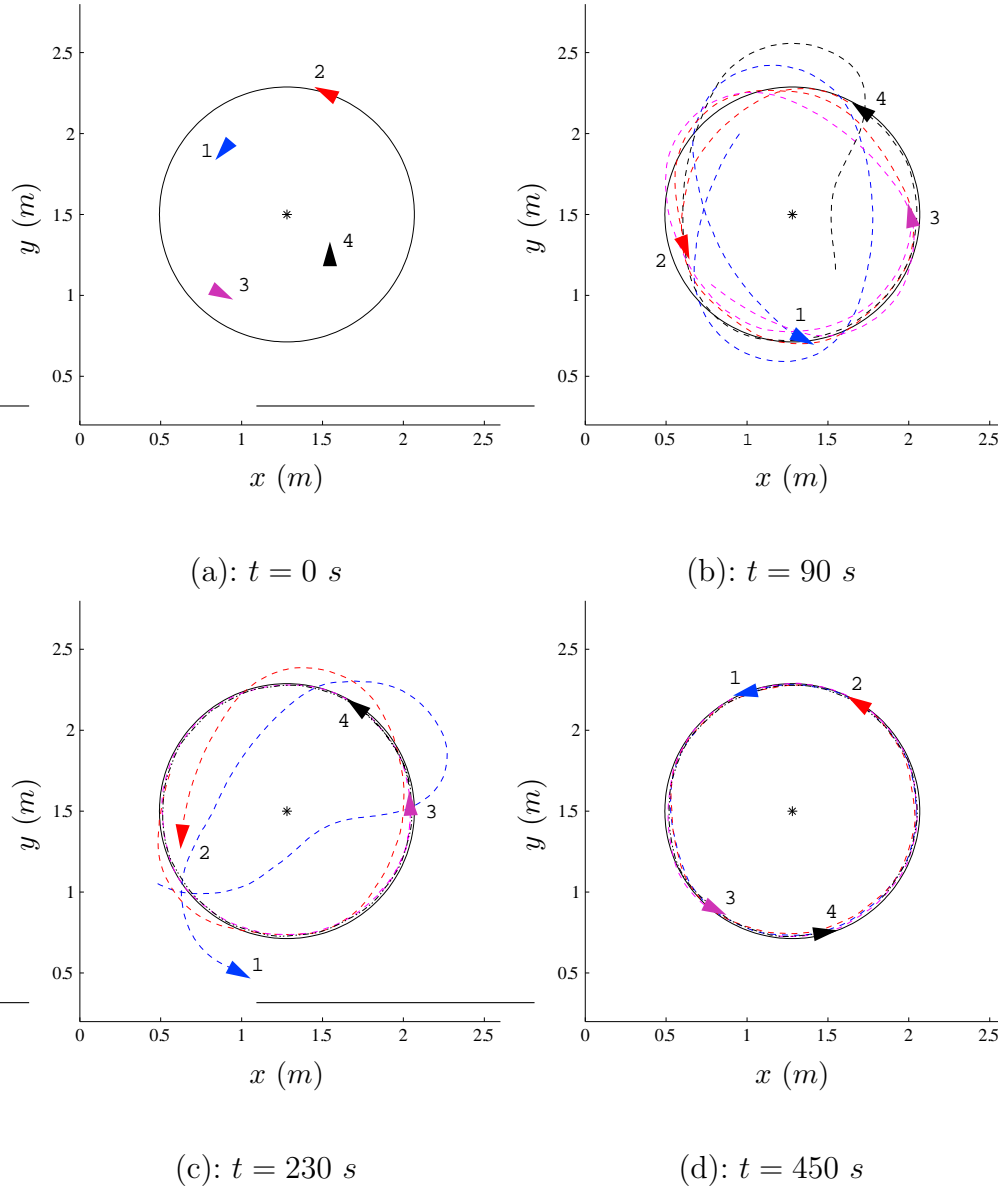


Fig. 12. Experiment B: Team configuration at different time instants. Dashed lines represent vehicle paths during the 90 seconds preceding each snapshot.

effective in avoiding collisions, also when considering the finite size of the vehicles (roughly enclosed in a circle of 0.1 m radius). The effect of the cross terms f_{ij} in the control law (3), and the role of the safety regions around each agent are clearly visible in Figure 9. When the vehicles come too close (see the initial part of the trajectories) the control inputs steer the agents away to prevent collisions.

A second set of experiments has been carried out with four vehicles, $\alpha_v = \pi/4$ and $d_0 = 0.7 \text{ m}$ (Experiment B). The controller parameters are the same as before except for $\rho_0 = 0.48 \text{ m}$. This choice satisfies all the stability constraints (see Figure 4), and results in a desired radius $\rho_e = 0.79 \text{ m}$. Figure 12 shows four

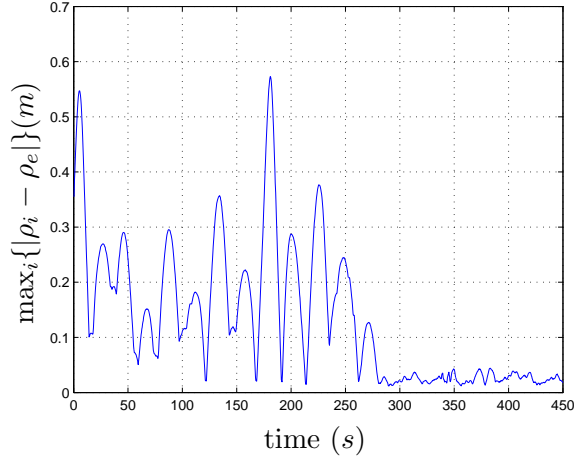


Fig. 13. Experiment B: Maximum deviation $|\rho_i - \rho_e|$ of vehicle distances to the beacon ρ_i , from the desired radius ρ_e .

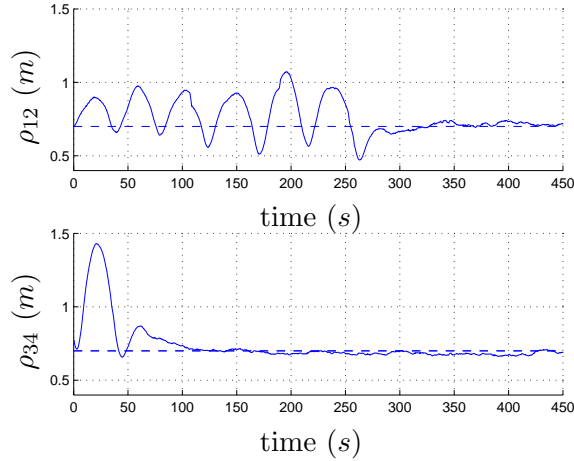


Fig. 14. Experiment B: Actual distances ρ_{12} , ρ_{34} between vehicles belonging to the same platoon (solid line), and desired one $d_0 = 0.7$ (dashed line).

snapshots of the team evolution during a typical run. In this experiment, the vehicles end up in rotating around the beacon in two separate platoons, each one made of two agents. After about 300 seconds, the motion of all the agents stabilizes on the desired circle, as shown in Figure 13. Moreover, the separation between vehicles belonging to the same platoon eventually approaches the desired value d_0 . In this case, agents 3 and 4 converge faster to the steady-state, than agents 1 and 2 (see Figure 14).

Several other experiments have been carried out over teams of 3 and 4 vehicles, with different visibility regions, controller parameters and initial vehicle poses. As expected, the final distribution of the robots in separate platoons depends on the initial configuration of the team, while the duration of the transient is mainly influenced by the number of robots in the team.

5.2 Moving beacon

A second experimental campaign has been carried out in order to evaluate the group behavior in case of moving beacon. As a matter of fact, although all the theoretical results have been obtained under the assumption of static reference beacon, numerical simulations have shown that the proposed control law is effective in achieving collective circular motion also in case of non stationary beacon [12]. To this purpose, two scenarios have been considered.

In the first one, the virtual beacon is allowed to instantaneously jump to a different position. The sequence of beacon locations can be thought of as a set of way points, about which the agents have to rotate at different time instants (e.g., a set of regions of interest or targets to be monitored). A similar scenario has been considered in [18], but employing two different control laws, one to enforce circular motion and one to track the new position of the beacon. Results of one of such tests are summarized in Figures 15-17 (Experiment C). The field of view of the simulated sensors and the controller parameters are the same as Experiment B, except for $d_0 = 0.4 \text{ m}$, $\rho_0 = 0.25 \text{ m}$, $k_b = 0.2$, resulting in a desired radius $\rho_e = 0.47 \text{ m}$. At the beginning of the experiment, the virtual reference beacon is located at position $(x, y) = (3.09, 4.63)$, and the two vehicles start from an initial configuration close to the equilibrium one. As long as the beacon does not move, the agents go on rotating on the desired circle (see upper-right circle in Figure 16). Suddenly, at $t = 109 \text{ s}$ the position of the virtual beacon switches to $(x, y) = (1.35, 1.35)$, thus pointing out that the target has changed (see Figure 15). As a consequence, both vehicles leave the circular trajectory and point straight toward the new beacon location (see linear stretch of the trajectories in Figure 16). After a transient, both vehicles eventually settle on the circle of desired radius centered at the new beacon location (see left-bottom circle in Figure 16). This is confirmed by Figure 17, where the distance of each vehicle to the reference beacon is shown. It is worth remarking that the transition between circular and linear motion performed by the vehicles is achieved without making any changes in the control law.

In the second scenario, the beacon acts as a moving target which must be tracked by the team. In Experiment D (carried out with the same controller parameters of Experiment C), the beacon is initially placed at $(1.74, 1.74)$, with the two vehicles rotating on the desired circle of radius $\rho_e = 0.47 \text{ m}$ (see left-bottom circle in Figure 19). After 53 s , the beacon starts moving straight at constant speed (0.0055 m/s), covering about 3.44 m in 630 s (see Figure 18). As a result, the agents keep on rotating about the beacon at roughly the desired distance ρ_e (see Figure 20), describing a circle translating according to the beacon motion. In this case, also the team cohesion is preserved, since the agents start in a single platoon and so remain during the whole experiment, with an actual inter-vehicle distance close to the desired one $d_0 = 0.4 \text{ m}$ (see

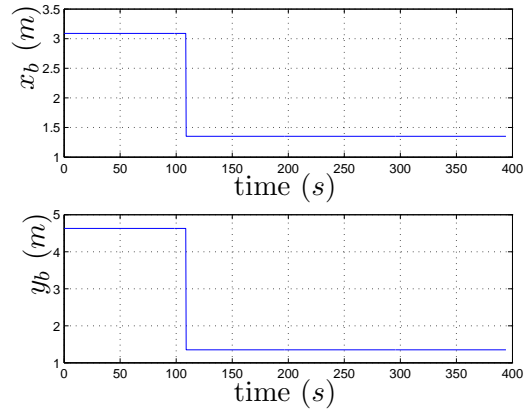


Fig. 15. Experiment C: Coordinates of the virtual reference beacon.

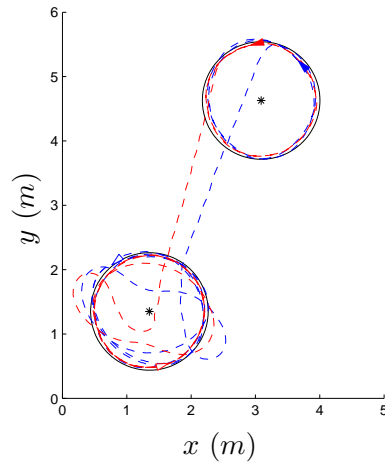


Fig. 16. Experiment C: Vehicle paths (dashed lines) and desired circular path (solid line) about the switching beacon (asterisks). Filled triangles represent the vehicle initial poses, empty triangles represent the final vehicle poses.

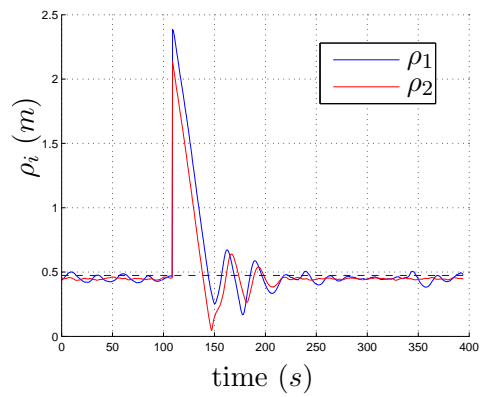


Fig. 17. Experiment C: Actual distances ρ_1 , ρ_2 of the vehicles to the switching beacon (solid lines) and desired radius $\rho_e = 0.47$ (dashed line).

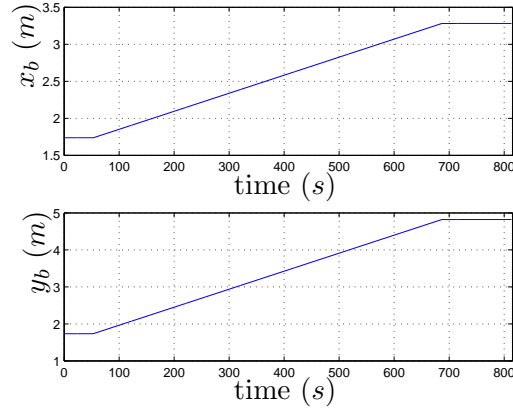


Fig. 18. Experiment D: Coordinates of the virtual reference beacon.

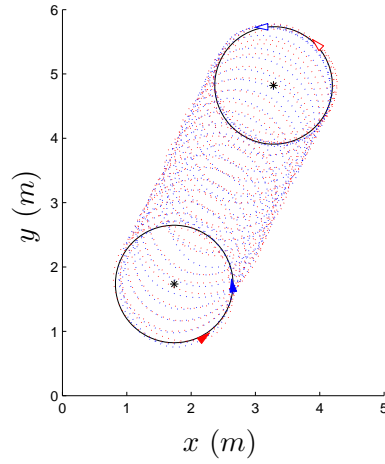


Fig. 19. Experiment D: Vehicle paths (dotted lines) and desired circular path (solid line) about the moving beacon (asterisks). Filled triangles represent the vehicle initial poses, empty triangles represent the final vehicle poses.

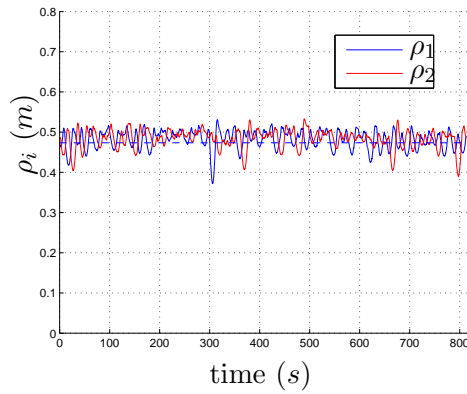


Fig. 20. Experiment D: Actual distances ρ_1 , ρ_2 of the vehicles to the moving beacon (solid lines) and desired radius $\rho_e = 0.47$ (dashed line).

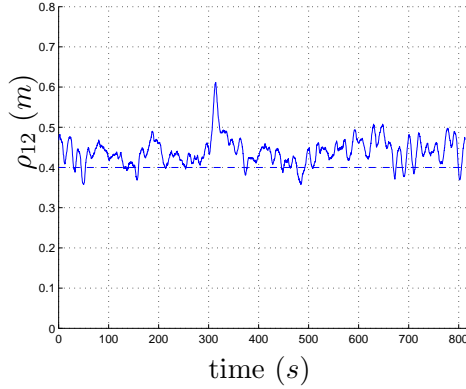


Fig. 21. Experiment D: Actual distance ρ_{12} between the vehicles (solid line) and desired one $d_0 = 0.4$.

Figure 21). Differently from the previous scenario (where the beacon jumped between different positions), in this case the agents are about 10 times faster than the beacon, thus allowing them to track it in circular motion.

This behavior suggests that by properly tuning the speed of the virtual reference beacon, it is possible to make the team show a variety of collective motions, ranging from rotation about a fixed point (Experiments A and B) to parallel linear motion (Experiment C), to rotation about a moving point (Experiment D).

The overall experimental validation has shown that the considered control law is fairly robust to a number of uncertainty sources and unmodeled effects arising in practice: poorly accurate measurements (due to the low resolution, uncalibrated camera), delays (due to image processing, IR communication between the central unit and vehicle controllers), nonlinear phenomena affecting the actuators (RCX numerical approximations, mechanical dead-zones).

6 Conclusions

In this paper, the experimental validation of a decentralized control law for the collective circular motion of nonholonomic vehicles has been presented. In spite of a quite challenging scenario (inaccurate measurements, communication delays, actuator saturations), promising results have been obtained, suggesting that the considered control strategy can be effectively applied in a real-world scenario. The adopted experimental setup provides a cost-effective solution for the validation of different control laws for multi-agent systems. In the case of a static reference beacon, the considered control strategy allows the team to achieve the desired collective circular motion, while at the same time avoiding collisions between agents. When tracking a moving beacon with

time-varying velocity profile, smooth transitions between circular and parallel motion have been observed, thus confirming the intuition underlying the design of the proposed control law.

Current lines of research include the theoretical analysis of the collective motion of the team in case of a moving reference beacon, and the design of novel control laws exploiting both the linear and the angular speed as control inputs of each vehicle. Finally, it is planned to adopt the same experimental setup to test and compare different control strategies.

References

- [1] A. Jadbabaie, J. Lin, and A. S. Morse. Coordination of groups of mobile autonomous agents using nearest neighbor rules. *IEEE Transactions on Automatic Control*, 48(6):988–1001, 2003.
- [2] N. E. Leonard and E. Fiorelli. Virtual leaders, artificial potentials and coordinated control of groups. In *Proceedings of the IEEE Conference on Decision and Control*, pages 2968–2973, Orlando, 2001.
- [3] Z. Lin, M. E. Broucke, and B. A. Francis. Local control strategies for groups of mobile autonomous agents. *IEEE Transactions on Automatic Control*, 49(4):622–629, April 2004.
- [4] J. A. Marshall, M. E. Broucke, and B. A. Francis. Formations of vehicles in cyclic pursuit. *IEEE Transactions on Automatic Control*, 49(11):1963–1974, November 2004.
- [5] E. W. Justh and P. S. Krishnaprasad. Equilibria and steering laws for planar formations. *Systems and Control Letters*, 52:25–38, 2004.
- [6] R. Sepulchre, D. A. Paley, and N. E. Leonard. Stabilization of planar collective motion with limited communication. *IEEE Transactions on Automatic Control*, 53(3):706–719, 2008.
- [7] A. K. Das, R. Fierro, V. Kumar, J. P. Ostrowski, J. Spletzer, and C. J. Taylor. A vision-based formation control framework. *IEEE Transaction on Robotics and Automation*, 18(5):813–825, October 2002.
- [8] J. A. Marshall, T. Fung, M. E. Broucke, G. M. T. D’Eleuterio, and B. A. Francis. Experiments in multirobot coordination. *Robotics and Autonomous Systems*, 54(3):265–275, 2006.
- [9] W. Ren and N. Sorensen. Distributed coordination architecture for multi-robot formation control. *Robotics and Autonomous Systems*, 56(4):324–333, 2008.
- [10] S. Mastellone, D.M. Stipanovic, C.R. Graunke, K.A. Intlekofer, and M.W. Spong. Formation control and collision avoidance for multi-agent non-holonomic

systems: Theory and experiments. *The International Journal of Robotics Research*, 27(1):107–126, 2008.

- [11] N. Ceccarelli, M. Di Marco, A. Garulli, and A. Giannitrapani. Collective circular motion of multi-vehicle systems with sensory limitations. In *Proceedings of the 44th Conference on Decision and Control*, Seville, Spain, December 2005.
- [12] N. Ceccarelli, M. Di Marco, A. Garulli, and A. Giannitrapani. Collective circular motion of multi-vehicle systems. *Automatica*, 44(12):3025–3035, 2008.
- [13] D. Benedettelli, N. Ceccarelli, A. Garulli, and A. Giannitrapani. Experimental validation of a decentralized control law for multi-vehicle collective motion. In *Proceedings of the 2007 IEEE/RSJ International Conference on Intelligent Robots and Systems*, pages 4170–4175, 2007.
- [14] LEGO MINDSTORMS. http://mindstorms.lego.com/eng/default_ris.asp.
- [15] K. Proudfoot. RCX internals. [Online]. Available: <http://graphics.stanford.edu/~kekoa/rcx/>.
- [16] M. L. Noga. BrickOS. [Online]. Available: <http://brickos.sourceforge.net>.
- [17] M. L. Noga. LNP, LegOS Network Protocol. [Online]. Available: <http://legos.sourceforge.net/HOWTO/x405.html>.
- [18] D. Paley, N. E. Leonard, and R. Sepulchre. Collective motion: bistability and trajectory tracking. In *Proceedings of the 43rd IEEE Conference on Decision and Control*, pages 1932–1936, Nassau, Bahamas, 2004.